Published online August 16, 2005

Assessing Contaminant Transport Vulnerability in Complex Topography Using a Distributed Hydrologic Model

Scott N. Martens and David D. Breshears*

ABSTRACT

Modeling of vadose zone hydrology is required to address a variety of applied problems in general and risk assessments associated with contaminants in particular. Risk assessments increasingly must focus on multisite, multipathway analyses as opposed to single-site, single pathway analyses. Such assessments can be particularly challenging when contaminants are widely dispersed in complex topography. Here we highlight how a set of contaminated sites situated within complex topography can be effectively prioritized relative to vulnerability of contaminant transport from surface and subsurface flows. We used a distributed hydrologic model, SPLASH, to assess the lateral flows of surface and subsurface water following the simulation of a 100-year precipitation event, which could correspond to an intense thunderstorm. Our case study was conducted in the North Ancho watershed of Los Alamos National Laboratory, in northern New Mexico, USA, an area with widely dispersed contaminants and diverse topography. Simulated surface flows generally exceeded subsurface flows by more than four orders of magnitude, indicating the relative importance of potential redistribution of contaminants by surface flows for this type of precipitation event. For the 18 potential contaminant release sites investigated, the maximum surface flow varied by more than an order of magnitude across the sites. Half of the sites had surface flows <25% of the maximum surface flow for a site, allowing for prioritization of those sites with the greatest vulnerability. Our results highlight how risks of contaminant transport can be effectively assessed in complex topography using distributed hydrologic modeling.

Modeling of vadose zone hydrology is required to address a variety of applied problems in general and risk assessments associated with contaminants in particular. Risk assessments related to the vulnerability of contaminant transport often focus on an individual site. Numerous models exist for such analyses, such as the RESRAD model, which is commonly used within the Department of Energy (DOE) (Cheng et al., 1991; Cheng and Yu, 1993; Wang et al., 1993; Yu et al., 1993a, 1993b; Wilcox and Breshears 1997). Such a modeling approach is useful for rapid and conservative assessments of risk from contaminants at a site. However, much of the contamination within DOE facilities is in low concentrations over widespread areas (Riley and Zachara, 1992). Some facilities, such as Los Alamos National Laboratory, have contaminants at widely scattered locations within a landscape of complex topography. This type of spatial distribution of contamination poses a particularly challenging problem for risk assessment. While many of the contaminated sites within an area of concern may have relatively low levels of contamination, the redistribution and concentration of these contaminants through environmental processes such as surface and subsurface flow must be considered (Wilcox et al., 1996a, 1996b, 1997; Wilcox and Breshears, 1997; Newman et al., 1998; Johansen et al., 2003). Because remediation associated with large areas of dispersed contaminants can be costly, assessments that can prioritize remediation resources and efforts on those sites with some combination of the highest concentrations and vulnerability to transport are greatly needed. Site contaminant inventories usually can be obtained with straightforward, albeit sometimes costly, sampling, whereas assessing the vulnerability of a site to contaminant transport is more challenging.

A major determinant of contaminant transport is the amount of hydrological flow at a given site. Vulnerability to contaminant transport can be associated with surface and subsurface flows of water laterally through a site. These flows themselves are influenced not only by the hydrologic characteristics of a site but also by the characteristics of nearby sites that may contribute or receive water flows. Data or predictions from a given location may or may not scale up to be relevant to larger scales of concern (Johansen et al., 2003; Wilcox et al., 2003a); hence the assessment of many locations may be needed. Assessing the relative magnitudes of surface and subsurface lateral flows can be particularly challenging in complex topography, where accounting for hydrology of surrounding sites may be crucial. Distributed hydrologic models provide a means for addressing these issues. Indeed, distributed hydrologic models have been applied to similar problems, such as prioritization of post-fire remediation efforts within burned areas in complex topography (Beeson et al., 2001; Wilson et al., 2001).

In this paper, we highlight the utility of a distributed hydrologic model for ranking vulnerability of different sites to contaminant transport by estimating relative magnitudes of surface and subsurface lateral flows across a complex landscape. More specifically, we used a distributed hydrologic model, SPLASH (Simulator for Processes on Landscapes: Surface/Subsurface Hydrology), to assess the lateral flows of surface and subsurface water following the simulation of a 100-yr precipitation event. This event was designed (McLin, 1992) to simulate a high-intensity rainfall event, which could correspond to an intense thunderstorm. Our case study was conducted in the North Ancho watershed of Los Alamos National Laboratory, in northern New Mexico, USA,

S.N. Martens, Department of Land, Air, and Water Resources, University of California at Davis, Davis, CA 95616 and Sierra Science, Three Rivers, CA 93271 (Present address); D.D. Breshears, Earth and Environmental Sciences Division, Mail Stop J495, Los Alamos National Laboratory, Los Alamos, NM 87545 and School of Natural Resources, Institute for the Study of Planet Earth, and Department of Ecology & Evolutionary Biology, University of Arizona, Tucson, AZ 85721-0043 (Present address). *Corresponding author (daveb@ag.arizona.edu).

Published in Vadose Zone Journal 4:811–818 (2005).
Special Section: Los Alamos National Laboratory
doi:10.2136/vzj2004-0037

677 S. Segoe Rd., Madison, WI 53711 USA

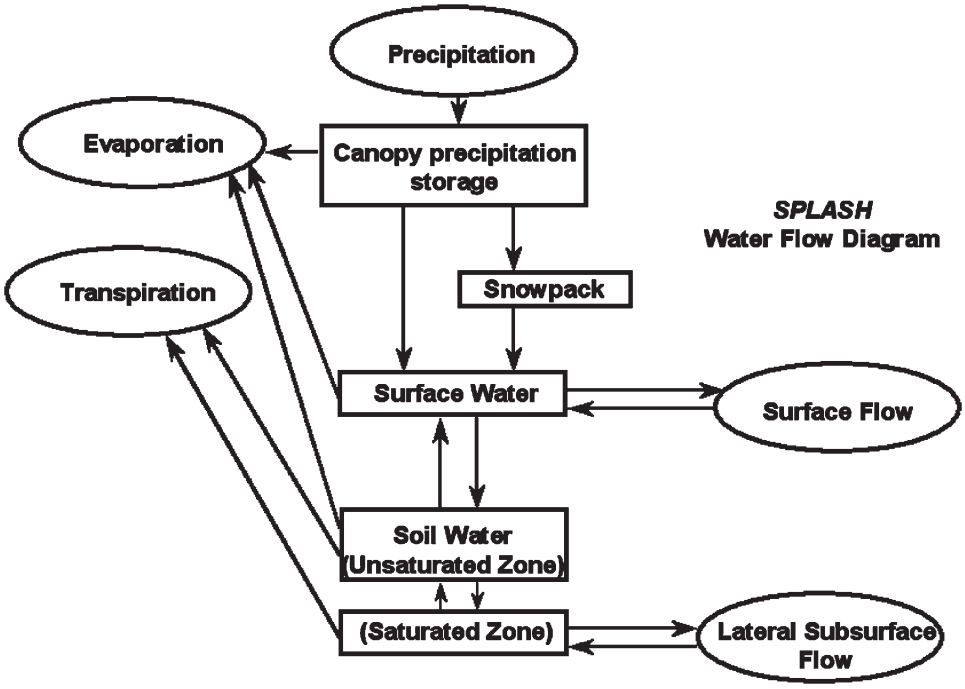

Fig. 1. Hydrological flows simulated by SPLASH.

an area with widely dispersed contaminants and diverse topography. The area around Los Alamos has been the focus of numerous hydrological field studies (e.g., Wilcox et al., 1997, 2003a, 2003b; Newman et al., 1998; Reid et al., 1999; Johansen et al., 2001, 2003) and modeling simulations (e.g., Beeson et al., 2001; McLin et al., 2001; Wilson et al., 2001), and hence this study further contributes to the larger body of research for Los Alamos and to making Los Alamos an important case study. Our results not only address site-specific needs, but more generally present an approach for assessing indices of vulnerability to redistribution by water for widely dispersed sites and highlight how risks of contaminant transport can be effectively assessed in complex topography.

METHODS

Hydrological Model

We conducted our analyses using SPLASH, a distributed simulation model that incorporates coupled surface–subsurface hydrology, lateral flow of surface and subsurface water, infiltration, evapotranspiration from a vegetation canopy, an energy balance approach for snowpack calculations, and a climate simulator (Martens, unpublished data, 2004; Beeson et al., 2001). For each cell within a grid, SPLASH calculates the components of a water budget through time including the flows of surface and subsurface water into and out of the cell. Because SPLASH explicitly calculates the lateral flows into and out of each cell for each time step of the simulation, it can produce a simulated hydrograph for each cell for both surface and subsurface lateral flows. The processes considered in SPLASH are shown in Fig. 1.

Three features of SPLASH are of particular relevance to this study: (i) lateral flows of surface water (e.g., runoff) are routed explicitly from a cell to its neighbors, (ii) subsurface lateral flow is calculated when the subsurface is saturated, and these flows are also routed explicitly from a cell to its neighbors, and (iii) the model has limited data input requirements. The primary spatially explicit inputs needed include digital maps of elevation, soil depths and textures, vegetation, and leaf area index (LAI).

In SPLASH, water that is ponded on the surface (often referred to as "surface head") may evaporate to the atmosphere, infiltrate into the soil below, and flow laterally to surrounding cells (and receive flows from surrounding cells). Note that infiltration and subsurface lateral flow are represented as separate processes in SPLASH and are not synonymous. The simulations presented here are driven by a brief, high-intensity rainfall event (described below) that exceeds the infiltration rate for many cells. This results in substantial ponding of surface water and subsequent lateral flow of this water across the topographically complex landscape.

SPLASH simulates lateral flow of ponded surface water using Manning's equation for calculating discharge from a cell. Water is routed in the direction of steepest descent (aspect) based on the digital elevation model (DEM). Water that is ponded on the surface (e.g., by saturation excess, infiltration excess) is subject to flow. Overland flow in SPLASH can be considered gradually varying sheetflow: the energy source for flow (gravity) is consumed by friction. The slope of the water surface is used to calculate the gradient between any two cells (diffusive wave approximation). (Optionally, the slope of the water surface may be assumed parallel to the bed [DEM] surface [kinematic wave approximation]). This allows SPLASH to simulate backwater effects and ponding of water in topographic depressions that may then overflow. However, SPLASH does not explicitly incorporate channel flow. Channel flow in SPLASH occurs only inasmuch as "channels" are defined by the DEM. SPLASH calculates water flow into or out of a cell through the four faces of that cell: two in the x direction, and two in the y direction. Velocities and discharges are calculated separately for each direction using Manning's equation. For example, in the x direction,

$$u = \frac{1}{n} h_s^{2/3} S_x^{1/2}$$

where u = velocity (m s^{-1}), n is Manning's roughness coefficient, h_s = hydraulic radius (m; which reduces to flow depth [surface head] for overland flow), and S_x = slope of surface head in the x direction (m m^{-1}). Discharge, Q (m^3 s^{-1}), is calculated as the product of velocity and cross-sectional area ($h_s \times$ cell size).

SPLASH calculates lateral saturated flow of subsurface water using Darcy's law which computes discharge, Q, as the product of saturated hydraulic conductivity, the gradient of hydraulic head, and saturated zone cross-section.

To allow for algorithmic simplicity, SPLASH uses an explicit, finite-difference calculation scheme. The timestep size, Δt, is dynamically determined based on a user-defined Courant number, c (where $0 < c \leq 1$; Courant et al., 1928), the cell size, x, and the maximum flow velocity on the grid at the previous timestep, v_{max}:

$$\Delta t = c(x/v_{max}).$$

It follows that if the maximum velocity is very large, the timestep must be correspondingly small. Because SPLASH has a minimum timestep size of 1 s, high flow velocities, which might occur in high-order channels, may cause numerical instability. To circumvent this possibility, a stream grid mask can be used by SPLASH, in which water is removed from each stream grid cell at each time step by setting h_s to zero for those cells at each time step (at the cost of having no simulation of "channel" flows in those cells).

Study Site and Data Inputs

Our case study was conducted for the North Ancho watershed, located at Los Alamos National Laboratory in northern New Mexico, USA. Major vegetation types included ponderosa pine (*Pinus ponderosa* Douglas) forest and piñon–juniper [*P. edulis* Engelm. and *Juniperus monosperma* (Engelm.) Sarg.] woodland, as well as disturbed areas from laboratory use. This drainage was selected because it contains several dispersed potential contamination release sites (PRS). The study area and associated potential contaminant release sites are shown in Fig. 2a. The potential contaminant release sites included landfill burial sites and firing sites for explosives testing, with contaminant types including high explosives and a variety of hazardous and radiological material.

We obtained a digital elevation map with 0.305-m horizontal resolution from the Facility for Information and Data Management (FIMAD) at Los Alamos National Laboratory. This map was resampled to create 30 by 30 m cells for a rectangular area of 122 cells north–south and 183 cells east–west, shown in Fig. 2b. We created elevation, slope, and aspect grids for input to SPLASH from these data. We also created a stream channel mask grid for use with SPLASH. This allows masking out stream channels from the computations of surface flow thus allowing faster processing (as described above).

A soil type map based on the survey of Nyhan et al. (1978) was also obtained from FIMAD and resampled to create 30 by 30 m cells. Soil descriptions in Nyhan et al. (1978) provided an estimated soil depth for each soil type. Where a mapped soil polygon included more than one soil type we assigned the characteristics of the areally dominant type to the whole soil polygon. For each described soil type we estimated percentages of sand, silt, and clay as the centroid for that textural class in the USDA soil texture triangle. We used the equations of Saxton et al. (1986) to estimate field capacity and saturated hydraulic conductivity for each soil type for input to SPLASH. For the SPLASH simulation, soil water content was initialized at 0.5 of field capacity for the soil profile. A vegetation map from FIMAD was also included and resampled to 30 by 30 m cells. We assumed a leaf area index (LAI) for each vegetation type, with LAI increasing such that grassland < savanna < woodland < forest. Spatially explicit estimates of LAI that vary within vegetation type can be derived and included in the analysis. LAI, however, is important when estimating transpiration and does not have a large effect on other simulated processes.

We conducted simulations for a storm of 100-yr frequency (McLin, 1992). We used estimates from the nearest meteorological station (located at Technical Area 59, Los Alamos National Laboratory) for 100-yr event amounts over 6-h periods (Table 3 in McLin, 1992). The time series for the cumulative storm distribution was taken from Table 2 in McLin (1992). The cumulative precipitation curve for the event is shown in Fig. 3. Note that the initial rates of precipitation are slow, which should lead to an increase in soil water content, followed by an enormous increase in precipitation intensity at 165 min after initiation of the storm. For this event, we ran the simulation for 24 h following the initiation of the event, which was at midnight during summer (June 29, chosen arbitrarily).

We summarized the results of our simulation of the 100-yr event by calculating the amount of water flowing through each cell during the 24-h period of the simulation (referred to as *total flow* or *total discharge* below). We calculated these values by integrating the discharge, Q, over the simulation period. We calculated total discharge for surface flow and for subsurface flow in each cell. The value indicates the amount of water that flowed into and out of a cell over the simulation and can be used as a relative index of vulnerability for water-driven contaminant mobility.

RESULTS

The amount of total surface flow varied over three orders of magnitude for the cells within the grid, as shown in Fig. 4. Some cells had total flows greater than the precipitation input because SPLASH routes flows through cells and these flows were integrated over the event to produce the values shown in Fig. 4. Most of the cells had total surface flows of less than 100 m^3, while a much smaller number of cells had much greater total surface flows, as shown in the histogram in Fig. 4 (note that the scale is log-log).

The predictions of surface water flows generated by SPLASH are sensitive to surface topography. Results in Fig. 5a illustrate how ponded water (surface head) has accumulated at the low-gradient area near the drainage outlet for a small (20 by 20 cells) subsection of the simulated area.

Although topography is a primary driver of surface flow, soil depth also influences surface flows, as illustrated in Fig. 5b. Cells with deep soils have a large profile water-holding capacity and do not generate as much surface flow in this simulation where the vadose zone water content was initialized at one-half of soil field capacity.

Indices of Site Vulnerability

The results of our simulation can be summarized with a vulnerability index for surface flow. For a vulnerability index we used the integrated discharge of surface water flow (m^3) passing through each 30 by 30 m cell during the simulation. The results are presented in Fig. 6a. The red

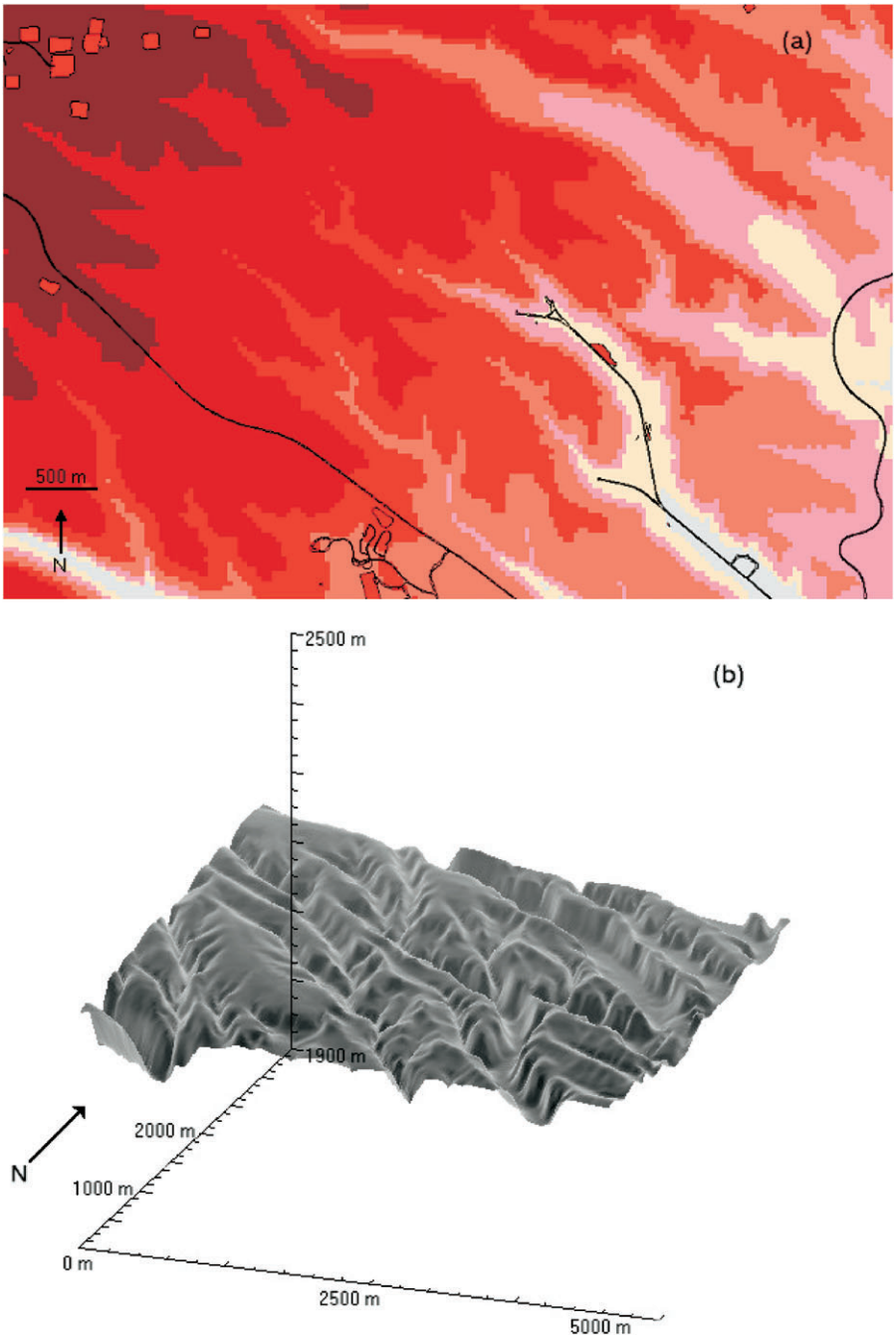

Fig. 2. (a) Color contour (40-m interval beginning at 1900 m) map of simulated area (5.5 km east–west by 3.6 km north–south) encompassing North Ancho watershed; potential contaminant release sites (PRSs) are shown as solid red polygons bordered by black line. (b) Shaded digital elevation model showing topography of simulated area (elevation range from 1907 to 2190 m), viewed from south-southeast; the North Ancho watershed is the set of drainages running diagonally through the area.

lines indicate the stream channel cells, which were masked out of the simulation. That is, water entering those stream cells was immediately removed from the simulation (as described earlier).

We calculated a similar index for subsurface lateral flow using the integrated subsurface discharge for each cell. The map (Fig. 6b) indicates regions of low and high subsurface lateral flow. Note however that the colors are again scaled from minimum to maximum, but in this case for subsurface flow. The magnitude of subsurface flow values was several orders of magnitude less than that for surface flow, so the pink color indicating zones of relatively high subsurface flow in this figure corresponds to much less water flow than the pink zones in the surface flow summary.

Data from these simulations were sorted to match the PRS sites of interest. We selected the maximum value of surface flow and the maximum value of subsurface lateral flow among all the cells within each PRS. These PRS sites were then ranked with respect to vulnerability in terms of surface flow (Table 1). Note that the maximum total surface flow for all of the PRSs is at least an order of magnitude less than the maximum for the entire simulated area (see Fig. 6).

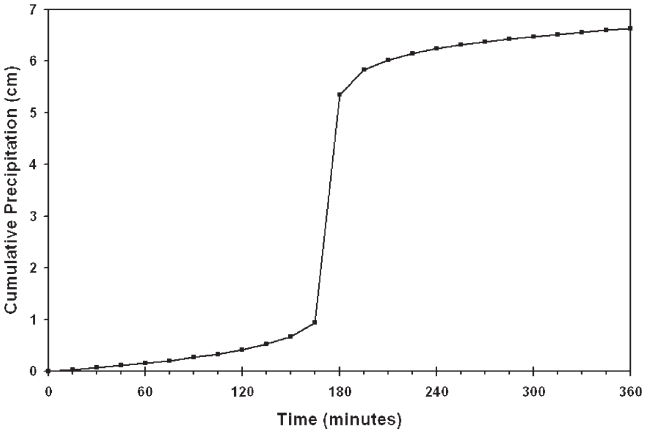

Fig. 3. Cumulative precipitation curve for 100-year event used in SPLASH simulations.

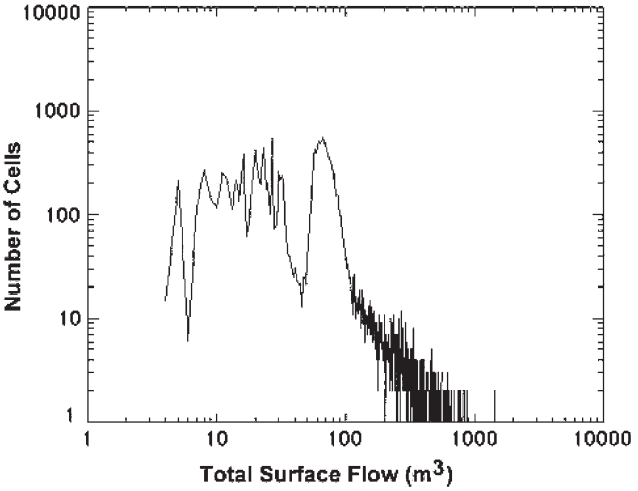

Fig. 4. Histogram (log-log) of total surface flow for each cell for the entire area simulated. Histogram bins are 1 m^3.

Similarly, the sites were ranked in terms of relative vulnerability to subsurface lateral flow (Table 1). Note, however, that the subsurface lateral flow is many orders of magnitude less than that for the surface flow. We expected little subsurface flow because the simulation was conducted for an extreme, high intensity precipitation event with soil water content initialized at 0.5 field capacity for the soil profile. This is not the scenario likely to generate maximum subsurface flow because soil was far from saturated initially, high intensity precipitation rates exceeded infiltration rates, and the simulation was for a short duration. Rather, maximum subsurface flow occurs when the soil profile is saturated. In the Los Alamos area, this is likely to happen following a series of snowmelt events, which result in a saturated soil profile (Wilcox et al., 1997; Wilcox and Breshears, 1997; Newman et al., 1998).

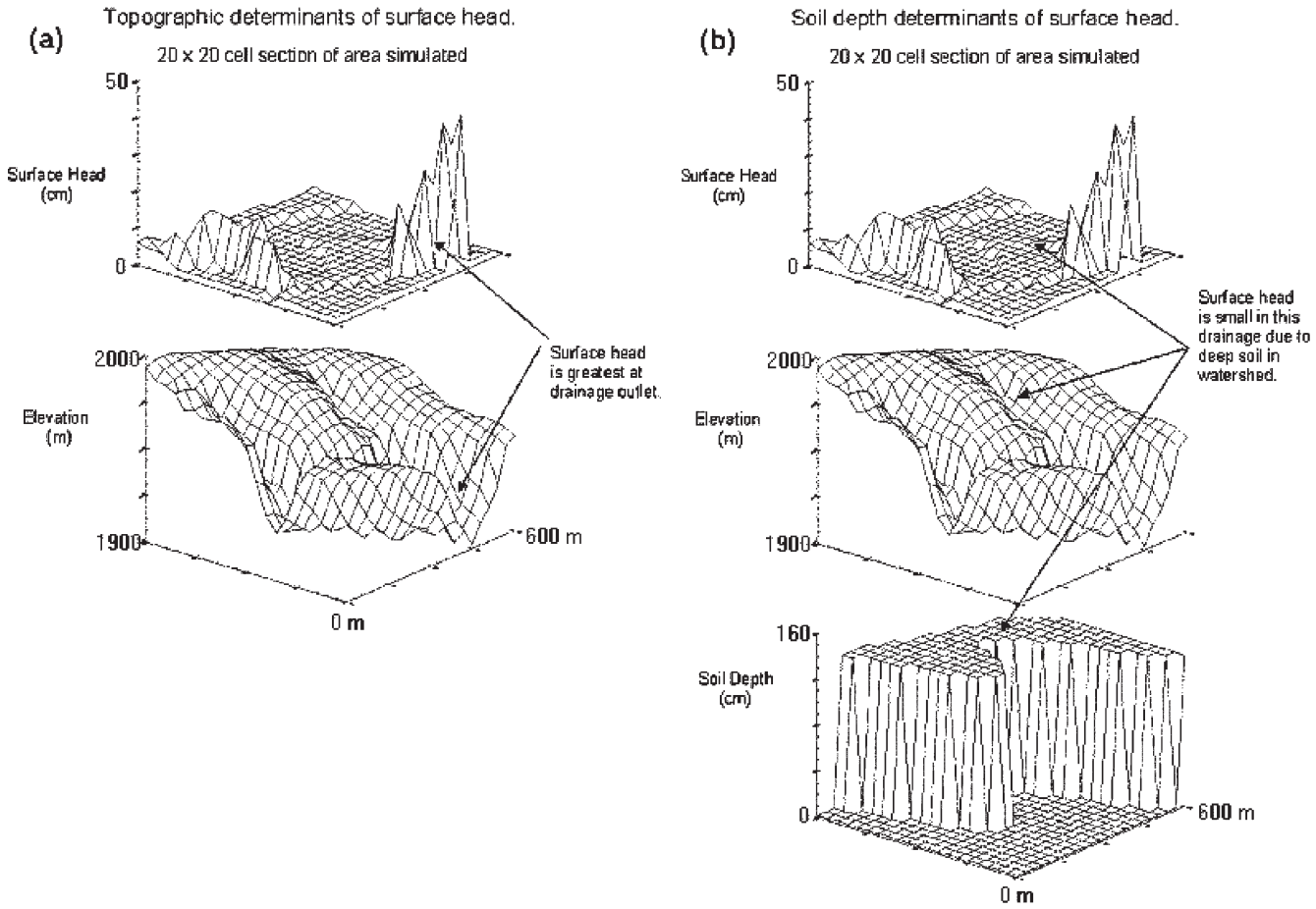

Fig. 5. (a) The effect of topography on surface runoff depth. (b) The effect of soil depth on surface runoff depth.

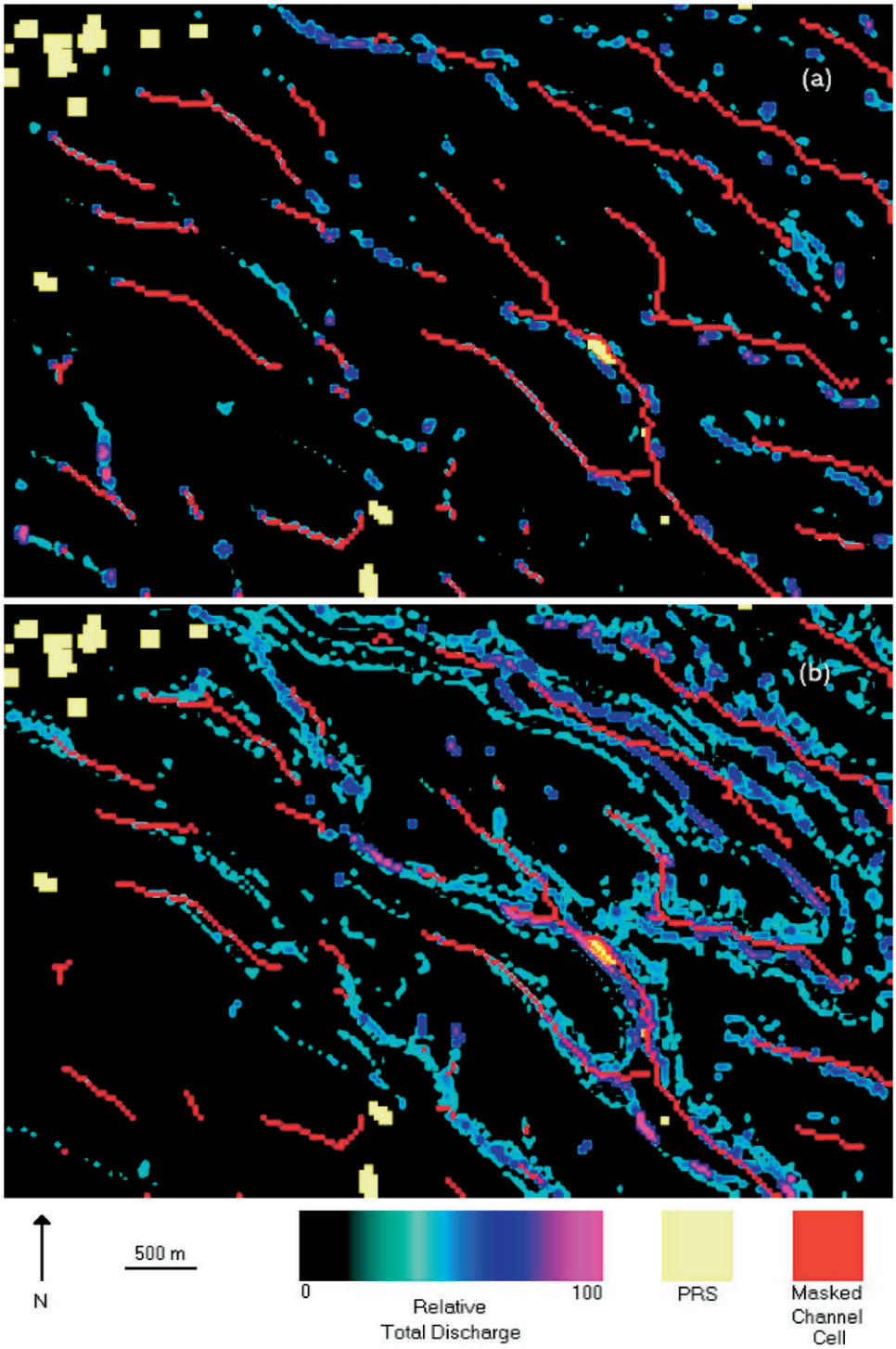

Fig. 6. (a) Normalized total surface flow amounts. The amount of flow passing through a cell is indexed as black < light blue < dark blue < pink, with pink being greatest. The values (0–100) are scaled relative to minimum and maximum flow calculated. The potential release sites (PRSs) are shown in yellow beneath the flow values; if there is no color on top of a yellow PRS, it indicates that no flow was generated at that cell. (b) Normalized total subsurface lateral flow amounts. The amount of subsurface lateral flow passing through a cell is indexed as black < light blue < dark blue < pink, with pink being greatest. The values (0–100) are scaled relative to minimum and maximum subsurface lateral flow calculated.

DISCUSSION

The results of our simulations provide a basis for assessing the relative vulnerability to transport of contaminants for a set of Los Alamos sites situated within complex terrain. We found that surface flows generally exceeded subsurface flows by more than four orders of magnitude, indicating the relative importance of potential redistribution of contaminants by surface runoff for this type of precipitation event. This finding is consistent with site-specific studies in that large subsurface flow events are only likely in ponderosa pine forests during warm periods following snowmelt (Wilcox et al., 1997;

Table 1. Total surface flow and total subsurface lateral flow for each potential release site (PRS) within the simulated area. For a PRS that covered more than one 30 by 30 m cell, the maximum value for any cell within the PRS was selected.

		Surface flow		Subsurface flow	
PRS number	PRS ID	Flow	Rank	Flow	Rank
		m^3		m^3	
49-008 (a)	1046	67.5	10	0	
49-001 (c)	1051	154.3	1	2.4×10^{-4}	3
49-008 (c)	1054	32.4	11	0	
49-001 (f)	1055	72.4	5	0	
49-001 (a)	1056	31.4	12	0	
49-002	1057	27.7	13	0	
C-00-036 (b)	1058	72.0	6	0	
49-001 (g)	1059	95.3	3	0	
49-001 (e)	1061	68.0	9	0	
49-005 (a)	1062	72.0	7	8.4×10^{-4}	1
49-008 (d)	1080	120.3	2	2.9×10^{-4}	2
49-007 (b)	1116	16.7	18	0	
C-00-036 (a)	1650	71.0	8	0	
36-001	1657	22.9	15	0	
39-001 (b)	1666	22.9	16	0	
39-007 (d)	1691	20.8	17	0	
Unnamed	2026	25.4	14	0	
C-00-037	2100	90.4	4	0	

Wilcox and Breshears, 1997; Newman et al., 1998) and are unlikely to occur in piñon-juniper woodlands (Wilcox et al., 2003a). Conversely, surface runoff has been shown to be important in both ponderosa pine forests (Wilcox et al., 1996a, 1997) and in piñon-juniper woodlands (Wilcox, 1994; Wilcox et al., 2003a). The amount of surface runoff and associated erosion is sensitive to the amount of surface cover and consequently can be further increased greatly following disturbances that reduce cover through drought, fire, or mechanical removal of vegetation (Wilcox 1994; Wilcox et al., 1996b, 2003a; Allen and Breshears 1998; Davenport et al., 1998; Johansen et al., 2001, 2003). Such disturbances, not accounted for in our simulations, would further amplify the differences between surface and subsurface flows.

Maximum surface flow was also highly variable among the 18 potential contaminant release sites that we investigated, varying by more than an order of magnitude across the sites. Half of the sites had surface flows <25% of that for the site with the greatest surface flow. Hence, these spatial differences among sites provide valuable, quantitative estimates of the potential vulnerabilities among sites to contaminant transport by surface flow. Again, the large degree of runoff is not surprising because studies in the area of interest have observed (Wilcox 1994; Wilcox et al., 1996b, 2003a; Johansen et al., 2001, 2003) or predicted (Beeson et al., 2001) this phenomenon. The site-specific rankings of potential vulnerability (Table 1) are useful at Los Alamos National Laboratory for prioritizing sites. Because subsurface flow is low, ranking sites based on surface runoff may be the most appropriate.

Our results highlight the value of using a distributed hydrologic model for ranking the vulnerability of contaminated sites in complex terrain. We were also able to evaluate the relative importance of surface vs. subsurface flow at a site. In our example, we evaluated risks for 18 potential release sites but in the process also evaluated hydrologic flows for a great number of locations. Hence, the approach demonstrated here can be used to evaluate any number of locations within the simulation domain. Indeed, in a previous analysis using SPLASH in an area compassing North Ancho, we evaluated all locations within the simulation with respect to surface flow to aide in prioritizing post-fire restoration efforts (Beeson et al., 2001). Evaluations of risks driven by hydrologic flows are important to a variety of problems, and so most generally, our results highlight how risks stemming from hydrologic flows in complex topography can be assessed using distributed hydrologic modeling.

ACKNOWLEDGMENTS

This work was supported by the Environmental Restoration Project at Los Alamos National Laboratory. We thank Brent Newman for comments on an earlier draft. D.D.B. completed revisions while at University of Arizona.

REFERENCES

Allen, C.D., and D.D. Breshears. 1998. Drought induced shift of a forest-woodland ecotone: Rapid landscape response to climate variation. Proc. Natl. Acad. Sci. USA 95:14839–14842.

Beeson, P.C., S.N. Martens, and D.D. Breshears. 2001. Simulating overland flow following wildfire: Mapping vulnerability to landscape disturbance. Hydrol. Process. 15:2917–2930.

Cheng, J.J., and C. Yu. 1993. Using the RESRAD computer code to evaluate human health risks from radionuclides and hazardous chemicals. J. Hazard. Mater. 35:353–367.

Cheng, J.J., C. Yu, and A.J. Zielen. 1991. RESRAD parameter sensitivity analysis. Environmental Assessment and Information Sciences Division, Report No. ANL/EAIS-3. Argonne Natl. Lab., Argonne, IL.

Courant, R., K.O. Friedrichs, and H. Lewy. 1928. Uber die partiellen differenzengleichngen der mathematishen physik. Mathematishe Annalen 100:32–74.

Davenport, D.W., D.D. Breshears, B.P. Wilcox, and C.D. Allen. 1998. Viewpoint: Sustainability of piñon-juniper woodlands—a unifying perspective of soil erosion thresholds. J. Range Manage. 51: 231–240.

Johansen, M.P., T.E. Hakonson, and D.D. Breshears. 2001. Post-fire runoff and erosion following rainfall simulation: Contrasting forests with shrublands and grasslands. Hydrol. Processes 15:2953–2965.

Johansen, M.P., T.E. Hakonson, F.W. Whicker, and D.D. Breshears. 2003. Pulsed redistribution of a contaminant following forest fire: Cesium-137 in runoff. J. Environ. Qual. 32:2150–2157.

McLin, S.G. 1992. Determination of 100-year floodplain elevations at Los Alamos National Laboratory. Report LA-12195-MS. Los Alamos Natl. Lab., Los Alamos, NM.

McLin, S.G., E.P. Springer, and L.J. Lane. 2001. Predicting floodplain boundary changes following the Cerro Grande wildfire. Hydrol. Process. 15:2967–2980.

Newman, B.D., A.R. Campbell, and B.P. Wilcox. 1998. Lateral subsurface flow pathways in a semiarid ponderosa pine hillslope. Water Resour. Res. 34:3485–3496.

Nyhan, J.W., L.W. Hacker, T.E. Calhoun, and D.L. Young. 1978. Soil survey of Los Alamos County, New Mexico. LA-6779-MS; UC-11. Los Alamos Natl. Lab., Los Alamos, NM.

Reid, K.D., B.P. Wilcox, D.D. Breshears, and L. MacDonald. 1999. Runoff and erosion for vegetation patch types in a piñon-juniper woodland. Soil Sci. Soc. Am. J. 63:1869–1879.

Riley, R.G., and J.M. Zachara. 1992. Chemical contaminants on DOE lands and selection of contaminant mixtures. Office of Energy Research, Washington, DC.

Saxton, K.E., W.J. Rawls, J.S. Romberger, and R.I. Papendick. 1986. Estimating generalized soil-water characteristics from texture. Soil Sci. Soc. Am. J. 50:1031–1036.

Wang, Y.-Y., B.M. Biwer, and C. Yu. 1993. A compilation of radionuclide transfer factors for the plant, meat, milk, and aquatic food pathways and suggested default values for the RESRAD code. Technical Report ANL/EAIS/TM-103. Natl. Tech. Info. Serv., Washington, DC.

Wilcox, B.P. 1994. Runoff and erosion in intercanopy zones of pinyon-juniper woodlands. J. Range Manage. 47:285–295.

Wilcox, B.P., C.D. Allen, B.D. Newman, K.D. Reid, D. Brandes, J. Pitlick, and D.W. Davenport. 1996a. Runoff and erosion on the Pajarito Plateau: Observations from the field, p. 433–439. *In* F. Goff, B.S. Kues, M.A. Rogers, L.D. McFadden, and J.N. Gardner. New Mexico Geological Society Guidebook, 47th Field Conf., Jemez Mountains Regions, Albuquerque, NM. 25–28 Sept. 1996. New Mexico Geological Soc., Albuquerque, NM.

Wilcox, B.P., and D.D. Breshears. 1997. Interflow in semiarid environments: An overlooked process in risk assessment. Hum. Ecol. Risk Assess. 3:187–203.

Wilcox, B.P., D.D. Breshears, and C.D. Allen. 2003a. Ecohydrology of a resource-conserving semiarid woodland: Effects of scale and disturbance. Ecol. Monogr. 73:223–239.

Wilcox, B.P., D.D. Breshears, and H.J. Turin. 2003b. Hydraulic conductivity in a piñon-juniper woodland: Influence of vegetation. Soil Sci. Soc. Am. J. 67:1243–1249.

Wilcox, B.P., B.D. Newman, D. Brandes, D.W. Davenport, and K. Reid. 1997. Runoff from a semiarid ponderosa pine hillslope in New Mexico. Water Resour. Res. 33:2301–2314.

Wilcox, B.P., J. Pitlick, C.D. Allen, and D.W. Davenport. 1996b. Runoff and erosion from a rapidly eroding pinyon-juniper hillslope. p. 61–77. *In* M.G. Anderson and S.M. Brooks (ed.) Advances in hillslope processes. Vol. 1. John Wiley & Sons, NY.

Wilson, C.J., J.W. Carey, P.C. Beeson, M.O. Gard, and L.J. Lane. 2001. A GIS-based hillslope erosion and sediment delivery model and its application in the Cerro Grande burn area. Hydrol. Process. 15:2995–3010.

Yu, C., C. Loureiro, J.-J. Cheng, L.G. Jones, Y.Y. Wang, Y.P. Chia, and E. Faillace. 1993a. Data collection handbook to support modeling the impacts of radioactive material in soil. Technical Report ANL/EAIS-8. Natl. Tech. Info. Serv., Washington, DC.

Yu, C., A.J. Zielen, J.-J. Cheng, Y.C. Yuan, L.G. Jones, D.J. LePoire, Y.Y. Wang, C.O. Loureiro, E. Gnanapragasam, E. Faillace, A. Wallo, III, W.A. Williams, and H. Peterson. 1993b. Manual for implementing residual radioactive material guidelines using RESRAD, Version 5.0. Technical Report ANL/EAD/LD-2. Natl. Tech. Info. Serv., Washington, DC.